Cuffless Hypertension Detection using Swarm Support Vector Machine Utilizing Photoplethysmogram and Electrocardiogram

Nuryani Nuryani (PhD)[1]*, Trio Pambudi Utomo (MSc)[2], Nanang Wiyono (MD)[3], Artono Dwijo Sutomo (MSc)[2], Steve Ling (PhD)[4]

[1]Department of Physics, University of Sebelas Maret Jl. Ir. Sutami 36A Kentingan Jebres Surakarta 57126, Indonesia
[2]Department of Physics, Graduate Program, University of Sebelas Maret Jl. Ir. Sutami 36A Kentingan Jebres Surakarta 57126, Indonesia
[3]Faculty of Medicine, University of Sebelas Maret Jl. Ir. Sutami 36A Kentingan Jebres Surakarta 57126, Indonesia
[4]Centre for Health Technologies, University of Technology Sydney, Broadway NSW 2007, Australia

ABSTRACT

Background: Hypertension is associated with severe complications, and its detection is important to provide early information about a hypertension event, which is essential to prevent further complications.

Objective: This study aimed to investigate a strategy for hypertension detection without a cuff using parameters of bioelectric signals, i.e., Electrocardiogram (ECG), Photoplethysmogram (PPG,) and an algorithm of Swarm-based Support Vector Machine (SSVM).

Material and Methods: This experimental study was conducted to develop a hypertension detection system. ECG and PPG bioelectrical records were collected from the Medical Information Mart for Intensive Care (MIMIC) from normal and hypertension participants and processed to find the parameters, used for the inputs of SSVM and comprised Pulse Arrival Time (PAT) and the characteristics of PPG signal derivatives. The SSVM was n Support Vector Machine (SVM) algorithm optimized using particle swarm optimization with Quantum Delta-potential-well (QDPSO). The SSVMs with different inputs were investigated to find the optimal detection performance.

Results: The proposed strategy was performed at 96% in terms of F1-score, accuracy, sensitivity, and specificity with better performance than the other methods tested and methods and also could develop a cuff-free hypertension monitoring system.

Conclusion: Hypertension using SSVM, ECG, and PPG parameters is acceptably performed. The hypertension detection had lower performance utilizing only PPG than both ECG and PPG.

Citation: Nuryani N, Utomo TP, Wiyono N, Sutomo AD, Ling S. Cuffless Hypertension Detection using Swarm Support Vector Machine Utilizing Photoplethysmogram and Electrocardiogram. *J Biomed Phys Eng*. 2023;13(5):477-488. doi: 10.31661/jbpe.v0i0.2206-1504.

Keywords

Photoplethysmography; Support Vector Machine; Medical Informatics

*Corresponding author:
Nuryani Nuryani
Department of Physics, University of Sebelas Maret Jl. Ir. Sutami 36A Kentingan Jebres Surakarta 57126, Indonesia
E-mail: nuryani@mipa.uns.ac.id

Received: 13 June 2022
Accepted: 11 January 2023

Introduction

Blood pressure is exerted on the vessel wall due to circulation. Hypertension is a condition characterized by elevated blood pressure. The seventh report of the Joint National Committee on prevention, detection, evaluation, and treatment of high blood pressure categorizes blood pressure as hypertension, prehypertension, and

normotension [1]. The report defined normotension as a systolic blood pressure of less than 120 mmHg and a diastolic blood pressure of less than 80 mmHg. The systolic and diastolic blood pressure range was 120-139 and 80-89 mmHg, respectively, for prehypertension. The hypertension category was separated into two stages: stage 1 (140-159 mmHg systolic and 90-99 mmHg diastolic) and stage 2 (more than 160 mmHg systolic and 100-110 mmHg diastolic).

The prevalence of hypertension is currently significant, and its global prevalence is projected to expand from 918 million to 1.56 billion between 2000 and 2025 [2]. A total of 26.4% of the global population had hypertension, with 26.1% of women and 26.6% of men affected [2]. It is predicted that 29.2% of the global population would have hypertension (29.0% of males and 29.5% of women) by 2025.

Uncontrolled hypertension may result in severe problems since it is a global risk factor for disability and mortality. Cognitive impairment was also linked to hypertension [3]. A strong association between high blood pressure and cardiovascular disease was also documented [4], and it was suggested that hypertension played a role in kidney disease [5].

Patients with hypertension should receive prompt therapy to reduce the occurrence of severe hypertension and its complications. It is vital to have timely information on hypertension-related events in a patient to provide early therapy [6]. It is possible to identify an episode of hypertension by measuring a patient's blood pressure with a blood pressure monitor, which typically employs an inflatable rubber bladder cuff. The strap is secured around the arm. Patients with a blood pressure cuff frequently experience discomfort due to the tightness of the inflated cuff.

In recent years, studies have focused on approaches or methods for measuring blood pressure without a cuff using an Electrocardiogram (ECG) and Photoplethysmogram (PPG) instead of a cuff [7]. A link was also reported between blood pressure and ECG and PPG parameters [8]. The PPG offered vital information regarding the cardiovascular system [9] with a new method for detecting hypertension by simplifying PPG characteristics, derived from PPG and the first and second derivatives.

The current study also introduces a Support Vector Machine (SVM) designed with a swarm approach to identify hypertension and compares its performance to that of other machine learning algorithms. The SVM is a suitable classification and a trustworthy machine-learning technique for a variety of applications [10, 11]. Quantum Delta-potential-well Swarm Optimization (QDPSO) [12] was employed to optimize SVM. The QDPSO as a novel algorithm is an enhanced variant of traditional PSO, influenced by quantum mechanics. In addition, the QDPSO updates the classical PSO rule, based on Newton's law.

Material and Methods

This experimental study was conducted to develop a hypertension detection system, which was developed and tested using bioelectrical signals, in hypertension and normotension states.

Dataset

This study used a database from Medical Information Mart for Intensive Care II (MIMIC II) provided by Physionet [13, 14]. The MIMIC II contained clinical data from tens of thousands of Intensive Care Units (ICU). The clinical data was acquired from hospital archives and workstations and comprised phycological signals with a duration of more than one day.

The database, including PPG, ECG (Lead II), and Arterial Blood Pressure (ABP) was collected. A total of 121 records were collected with good quality signals and 120 s in length [15]. The blood pressure was represented by the ABP and categorized as normotension, prehypertension, and hypertension based on the Seventh Report of the Joint National

Committee (JNC 7) [1]. A total dataset of 17,534 consisting of 6,229, 5,079, and 6,232 was used for normotension, prehypertension, and hypertension, respectively. The dataset was then randomly split for training and testing for five-fold cross-validation, in which 80% and 20% of the dataset were for training and testing, respectively.

Detection System of hypertension

The general design of the proposed hypertension detection system is presented in Figure 1. The signals were ECG and PPG as the inputs of the detection system. Feature extraction was created to find five ECG-PPG features, i.e., PAT (Pulse arrival time), D1, A1, D2, and D2. The PAT was from both ECG and PPG, and the other features were from PPG alone, as follows:

D1: The distance between the PPG peak and the minimum point of the PPG first derivative.

D2: The distance between the PPG peak and the maximum point of the PPG's second derivative.

A1: The area under the PPG curve between a PPG peak and the minimum point of the PPG first derivative.

A2: The detail of the features is presented in the next section.

Subsequently, the features were fed to the SSVM-based classifier, which was optimized using QDPSO. The output of the detection system was the category of blood pressure: normal or hypertension. The design was implemented using Python programming language (3.7.0).

Feature extraction

Feature extraction was used to find the five features, as presented in Figure 2: Pulse Arrival Time (PAT), D1, D2, A1, and A2 [15]. The PPG peak was called as systolic peak and the minimum of the PPG first derivative was called as diastolic peak [16]. A1 was the area under the PPG curve between a PPG peak and the minimum point of the PPG first derivative; D2 was the distance between the PPG peak and the maximum point of the PPG's second derivative, and A2 was the area under the PPG curve between a PPG peak and the maximum point of the PPG's second derivative.

The position of the QRS peak was necessary as the starting point to get PAT. Some steps are necessary to find the QRS peak as follows: firstly, applying low-pass and high-pass filters to the ECG with cut-off frequencies of 20 Hz and 5 Hz, respectively; secondary, Moving Wave Integration (MWI) were applied using Mexican Hat wavelet [17] and squaring process. During MWI, the local maxima points

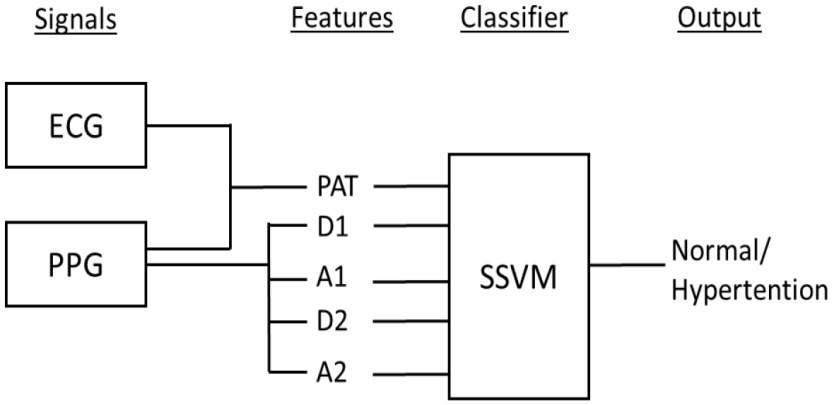

Figure 1: The design of a hypertension detection system using SSVM (support vector machine) with the features of ECG (electrocardiogram) and PPG (photoplethysmogram): PAT (pulse arrival time), D1, A1, D2, and A2

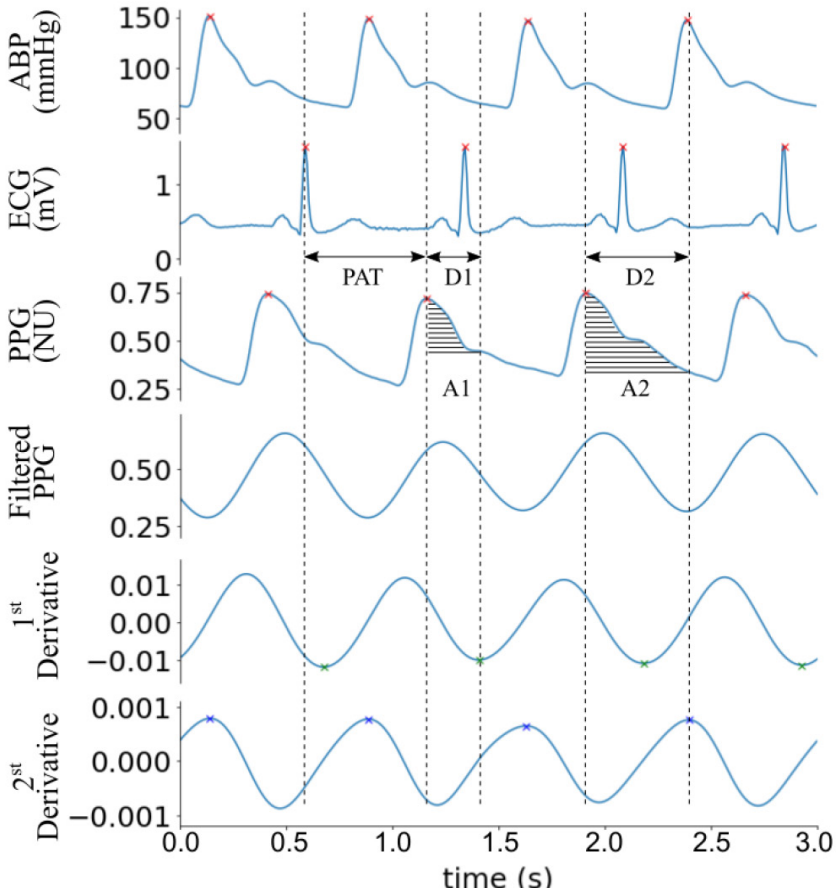

Figure 2: The definition of ECG (electrocardiogram) and PPG (Photoplethysmogram) features. Pulse Arrival Time (PAT), D1, D2, A1, and A2, and the associated Atrial Blood Pressure (ABP) signal. ECG-PPG (electrocardiogram-Photoplethysmogram) is presented in Normalized Unit (NU).

were iterated and checked. A maxima point was defined as QRS-complex if it exceeded a defined threshold and came after a refractory period (0.2 s). Otherwise, it was defined as a noise peak. If no QRS complex was detected within a defined period (T), a back-search algorithm was conducted using a lower threshold. The T was defined as follows:

$$T=1.66\times RR \qquad (1)$$

where RR was the time length between two consecutive QRS peaks.

The end of PAT was the PPG peak position on the right side of the QRS peak, and the PPG peak is found as follows: 1) applying the 4th of Chebyshev type II for filtering, 2) creating a moving window, and 3) defining the largest point in this window as the PPG peak with the window size of 61 samples.

Support Vector Machine (SVM)

The SVM constructed an optimal hyperplane that separated binary class data. Training data, $X=(x_i,y_i)$, was linearly separated, where $x_i \in \mathbb{R}^m$ was a m-dimensional space, and y_i was the class label, i=1,2, …, k, k was the amount of data. Support vectors were training data that satisfied,

$$y_i(w.x+b)-1\geq 0 \qquad (2)$$

and laid in the equality of the equation. $w.x+b=0$ was optimal hyper-parameter; w

was the hyperplane perpendicular vector; and b was bias or threshold. The optimum hyperplane was determined by maximizing the margin between two hyper-planes: $w.x+b=+1$ and $w.x+b=-1$. The margin between these two hyper-planes was $2/\|w\|$.

Such separating hyperplanes did not exist in many real-world problems. Therefore, a slack variable ζ_i was inserted and then $y_i(w.x+b)\geq 1-\zeta_i$. The optimal separating hyperplane was determined by minimizing.

$$C\sum_{I=1}^{k}\zeta_i+\frac{1}{2}\|w\|^2 \quad (3)$$

C was a *cost* constant to control the trade-off between error and margin size. The optimal hyperplane can be found by performing a large range multiplier approach by maximizing;

$$L(\alpha)=\sum_{i=1}^{k}\alpha_i-\frac{1}{2}\sum_{i=1}^{k}\sum_{j=1}^{k}\alpha_i\alpha_j y_i y_j\left(x_i.x_j\right) \quad (4)$$

subject to $0\leq\alpha_i<C$ and $\sum_{i=1}^{k}y_i\alpha_i$ where α_i was the Lagrange multiplier. Imbalanced data between two classes often happened in real data. Therefore, a higher error weight (w_0 or w_1) was given to the class that had a smaller population. Then equation (1) was modified by minimizing.

$$w_0C\sum_{i:y_i=-1}^{k}\zeta_i+w_1C\sum_{i:y_i=+1}^{k}\zeta_i+\frac{1}{2}\|w\|^2 \quad (5)$$

The inner product in equation (3) was substituted by a kernel function $K(x_i,x_j)$ to map the input to space with a higher dimension. The mapping made the non-linearly separable data to be able for linear classification. We adopted the Radial Basis Function (RBF) for the function. RBF was defined as;

$$K\left(x_i,x_j\right)=exp\left(-\gamma\|x_i-x_j\|^2\right) \quad (6)$$

The prediction result for any test vector $x\in\mathbb{R}^N$ was defined by,

$$f\left(x\right)=sgn\left(\sum\alpha_i y_i k\left(x_i,x\right)+b\right) \quad (7)$$

sgn was a signum function. Using the signum function, the $f(x)$ value of more than 0 was defined as +1 class, otherwise, it was defined as -1 class.

Quantum Delta Particle Swarm Optimizer (QDPSO)

It was assumed that the particle position at search step l was s_l, at step l+1, and the particle might be in the zone of (-|h|,|h|) with a probability of z, or out of the zone with the probability 1-z. s converged to the center point, p, if we set z>0.5. Thus, the probability h_{l+1} on the left side of $|h_l|$ must be more than 0.75. Therefore, the length of Delta L was obtained as follows:

$$\begin{aligned}1>\int_{-\infty}^{|h_l|}Q(h)\,dh=\int_{-\infty}^{|h_l|}\left|\psi(h)\right|^2 dh\\ =\int_{-\infty}^{|h_l|}\frac{1}{L}e^{-2|h|/L}dh=0.5+\int_{0}^{|h_l|}\frac{1}{L}e^{-2h/L}dh\\ =1-\frac{1}{2}e^{-2|h_l|/L}>0.75\end{aligned} \quad (8)$$

Where $Q(h)=|\psi(h)|^2$ was probability density function,

$$\begin{aligned}e^{2|h_l|/L}>2\\ L<\frac{1}{ln\sqrt{2}}|h_l|=\frac{1}{ln\sqrt{2}}|s_l-p|\end{aligned} \quad (9)$$

L was formulated as $L=(1/g)|s_l-p|$ and g was a parameter constrained by.

$$g>ln\sqrt{2} \quad (10)$$

The control parameter L can reduce to the control and selection of parameter g. The QDPSO algorithm was described as follows (Figure 3) [12].

Results

This section presents the ECG/PPG features in different blood pressure categories and the hypertension detection performances using SSVM and other methods. The performances are presented in terms of F1-score [15, 18].

The ECG/PPG features in three categories of blood pressure are presented in Table 1, in the forms of mean and standard deviation. The PAT, A2, and D1 were higher during normotension than in prehypertension and hypertension. All features were higher in hypertension than in prehypertension. In addition, each

QDPSO pseudocode

Initialize population: s

for i= 1 to population size M:

if $f(s_i) < f(p_i)$:

$$p_i = s_i$$

$$p_g = min(p_i)$$

for d = 1 to dimension D

$$\phi_1 = rand(0,1) \text{ and } \phi_2 = rand(0,1)$$

$$p = (\phi_1 * p_{id} + \phi_2 * p_{gd})/(\phi_1 + \phi_2)$$

$$u = rand(0,1)$$

$$L = (1/g) * |(s_{id} - p)|$$

if $rand(0,1) > 0.5$:

$$s_{id} = p - L * (ln(1/u))$$

else:

$$s_{id} = p + L * (ln(1/u))$$

Figure 3: Quantum Delta Particle Swarm Optimizer (QDPSO) algorithm

Table 1: ECG (Electrocardiogram)/PPG (Photoplethysmogram) features in three categories of blood pressures

Features	Normotension	Prehypertension	Hypertension	ANOVA *P*-value
PAT	0.50±0.23	0.41±0.26	0.48±0.22	<0.0001
A1	0.04±0.04	0.03±0.02	0.04±0.03	<0.0001
A2	0.10±0.09	0.06±0.03	0.09±0.06	<0.0001
D1	0.22±0.05	0.21±0.06	0.21±0.04	<0.0001
D2	0.47±0.14	0.44±0.16	0.47±0.16	<0.0001

PAT: Pulse Arrival Time

feature significantly differed in the three categories, considering the *P*-values.

The performances of SSVM using three different Feature Sets (FS) in three various trials consisting of Trial-A (normotension vs prehypertension), Trial-B (normotension vs hypertension), and Trial-C (normotension-prehypertension vs hypertension) as seen in Table 2. Three feature sets comprised FS1 (PAT, D1, A1), FS2 (D1, A1, D2, A2), and FS3 (PAT, D1, A1, D2, A2). The performance was measured in terms of F1-Score, accuracy, sensitivity, and specificity.

The detection performances were almost

Table 2: The performances of hypertension detections using SSVM (Support Vector Machine) with three different trials using three different feature sets.

Trial	Feature Sets	F1-Score (%)	Accuracy (%)	Sensitivity (%)	Specificity (%)
Trial-A (Normotension vs Prehypertension)	FS1	87.04	87.14	85.57	88.47
	FS2	87.95	88.06	85.95	89.83
	FS3	93.58	93.63	92.46	94.62
Trial-B (Normotension vs Hypertension)	FS1	91.55	91.55	91.58	91.51
	FS2	91.44	91.44	91.48	91.41
	FS3	96.50	96.50	96.40	96.59
Trial-C (Normotension-Prehypertension vs Hypertension)	FS1	88.08	89.07	84.52	91.59
	FS2	88.56	89.58	83.72	92.83
	FS3	93.76	94.32	90.50	96.43

Feature FS1: PAT (Pulse Arrival Time), D1, A1

Feature FS2: D1, A1, D2, A2

Feature FS3: PAT, D1, A1, D2, A2

the same in all the trials, in all four terms of performances using FS1 and FS2. For trial-B, the F1-scores were 91.55% and 91.44% for FS1 and FS2, respectively. The detection, which used FS3, performed higher than that used FS1 and FS2. The SSVM provided the highest performance in Trial-B with FS3, resulting in F1-score, accuracy, sensitivity, and specificity of 96.49%, 96.50%, 96.40%, and 96.59%, respectively. The SSVM which used FS1 and FS2 performed lower with all terms of about 91%.

The performance of the proposed method is presented in Table 3 and compared to other studies. Four algorithms: Logistics Regression, AdaBoost Tree, Bagged Tree, and k-nearest neighbors (KNN) were studied for hypertension detection [15] using PAT and 10 PPG features. These algorithms also carried out the three trials, as the proposed method did. As presented in Table 3, the performances of these algorithms were lower than SSVM (the proposed method). Among those four algorithms, KNN performed the highest in terms of F1-score. For Trial-B with PAT and 10 PPG features, this KNN obtained F1-Score of 94.84%, lower than SSVM's performance, of 96.49%.

The proposed method also outperformed the GoogleNet algorithm [19]. For Trial-B with Continuous Wavelet Transform (CWT) scalogram, the GoogleNet performed 92.55%. Moreover, hypertension detection using SVM without QDPSO was also studied. This SVM with PAT and 4 PPG features performed 94.58% for Trial-B. Multilayer Perceptron (MLP) was also investigated. The MLP resulted in the performance of 93.47% for Trial-B, lower than SSVM using PAT and four PPG features.

Discussion

This article introduces a strategy for hypertension detection using SSVM and ECG-PPG features. The SVM as a famous machine learning is used for applications in various fields, such as healthcare [10, 20], agriculture [21], manufacturing [22], and finance [23]. Prior studies reported the superiority of SVM over other methods [24].

The optimal SVM hyperparameters *C* and gamma were needed to obtain an SVM with

Table 3: Performance comparison of SSVM (Support Vector Machine) and other methods

Trial	Features	Classifiers	F1-Score (%)
Trial-A	PAT and 10 PPG features	Logistic Regression by [15]	63.92
Trial-B			79.11
Trial-C			62.26
Trial-A	PAT and 10 PPG features	AdaBoost Ttee by [15]	74.67
Trial-B			90.15
Trial-C			79.71
Trial-A	PAT and 10 PPG features	Bagged Tree by [15]	83.88
Trial-B			94.13
Trial-C			88.22
Trial-A	PAT and 10 PPG features	KNN by [15]	84.34
Trial-B			94.84
Trial-C			88.49
Trial-A	CWT Scalogram	The The The GoogleNet [19]	80.52
Trial-B			92.55
Trial-C			82.95
Trial-A	PAT and 4 PPG features	MLP	90.71
Trial-B			93.47
Trial-C			87.54
Trial-A	PAT and 4 PPG features	SVM	90.71
Trial-B			94.58
Trial-C			92.68
Trial-A	PAT and 4 PPG features	SSVM	93.38
Trial-B			96.49
Trial-C			93.76

PAT: Pulse Arrival Time, PPG: Photoplethysmogram, KNN: K-Nearest Neighbors, CWT: Continuous Wavelet Transform, MLP: Multilayer Perceptron, SVM: Support Vector Machine, SSVM: Swarm Support Vector Machine

good performance. The optimal values could be obtained using the grid search algorithm [25], in which the search space of parameters is divided into groups of possible parameters for testing. Alternatively, a global optimization algorithm can be used to find the optimal hyperparameters, such as particle swarm optimization (PSO). This study used an enhanced PSO, QDPSO, forming SSVM. Theoretical and experimental studies showed that QDPSO outperformed the traditional PSO [12]. The hypertension detection performance improved F1-score from 94.58% to 96.49%, and the hypertension detection performance was 96.49%, higher than when the SVM was without optimization, at 94.58% using SSVM.

The hypertension detection using the proposed SSVM performed higher than the GoogleNet [19]. The GoogleLeNet was a convolutional neural network that had been extended with deeper architectures [26]. In the hypertension detection method using the GoogleNet, a transformation of PPG signals with a continuous wavelet transform (CWT)

was used for the input of the GoogleNet. The transformation aimed to convert the PPG signals to Red-Green-Blue (RGB) images.

The hypertension detection using the proposed SSVM also performed higher than that of the classification algorithms, such as AdaBoost Tree, Bagged Tree, Logistic Regression, and KNN [15] that represented different classification theories, such as bagged decision tree, regression, and clustering. The Bagged Tree and the KNN outperformed the GoogleNet. Furthermore, in SVM without any optimization, the hyperparameters outperformed Multilayer Perceptron (MLP), a type of Artificial Neural Network (ANN).

The present study includes PPG features for hypertension detection. Essentially, PPG comprises infrared light to estimate the volumetric alteration of blood circulation and can depict important information about the cardiovascular system [27]. The initial functions of PPG aimed to measure heart rate and pulse oximetry. Further studies are conducted to explore other valuable information from PPG, such as arteriosclerosis and vascular aging [28-31].

One cycle of PPG comprises two parts, showing systolic and diastolic components [32], represented by the left and the right sides, respectively, of the PPG peak. The systolic part shows the pressure transmission from the aortic root to the finger. Moreover, the diastolic part indicates the pressure transmitted from the ventricle to the lower body, reflected along the aorta to the finger.

The PPG parameters extracted from the derivative of PPG signals were included, and the first and second derivatives were used in the current study. The derivative could be used to obtain more detailed information about the original PPG signal. For example, feature D1 (Figure 1) represented the period between the PPG peak and the minimum of the PPG first derivative, which coincided with the diastolic peak of the original PPG. Therefore, D1 represented the period between the PPG peak and the diastolic peak. The feature A1 represented the area under the curve D1. In clinical studies, the area under curve is frequently used as an indicator [33, 34].

Recently, the second derivative of PPG is favorable for researchers to estimate vascular aging [35], arterial distensibility [36], heart rate variability [37], the risk of coronary heart disease in the general population [38], and other clinical problems.

The ECG-PPG features utilized in this proposed method consisted of four PPG-features and one feature from ECG-PPG. All the features were extracted from time-domain signals instead of frequency or other more complicated forms. The processes for locating the features were not overly complicated. The main process for ECG processing was to identify QRS-peaks, which was a well-known process with many alternative algorithms available [39]. For the PPG processing, it just needed to find the first and second derivatives of the PPG signal and get the maximum and minimum of these derivatives. Methods to find the derivative, maximum, and minimum of the signal were basic computational algorithms [40]. The uncomplicated process can be easily reproduced and implemented in a real-time application.

The MIMIC dataset was used with records containing ABP, ECG (II), and PPG. The ABP and PPG records, in which their systolic and diastolic waves' morphology cannot be distinguished and are highly distorted, were not used. Besides, the ECG records with distorted QRS-complex peaks were also not used. Finally, 121 records with a 120-second length signal were found for each record.

Hypertension detection using only PPG can provide advantages in terms of simplicity. However, the detection using only PPG still provided lower performance than that used both ECG and PPG. The lower performance of which used PPG only also reported in [19]. Therefore, further studies are still needed to increase the performance of hypertension detection using only PPG. The reasons to

select PPG alone are low cost, easy to use, easy implementation, and non-invasiveness.

Conclusion

A cuffless method was introduced for hypertension detection using a swarm-based SSVM algorithm and ECG-PPG. SSVM was an SVM optimized using QDPSO. In this hypertension detection, SSVM outperformed various machine learning algorithms. ECG, original PPG, and the first and the second derivatives of PPG significantly contributed to hypertension detection. SSVM using ECG and PPG had an adequate performance for hypertension detection, with an F1-Score of 96.49%. However, hypertension detection showed low performance utilizing PPG only. Further studies to find a method for hypertension detection, which uses PPG alone, are still needed to improve the performance.

Authors' Contribution

N. Nuryani contributed to the general design and algorithm of the detection system. TP. Utomo implemented the algorithm. N. Wiyono analyzed the clinical data. AD. Sutomo prepared input data. S. Ling provided the optimization. The preliminary article was presented by N. Nuryani and was followed up by a discussion with the others. All the authors read and approved the final version of the manuscript.

Ethical Approval

The study utilized the publicly available dataset from MIMIC (Multiparameter Intelligent Monitoring in Intensive Care), for which ethical approval has been provided previously by the Institutional Review Boards of BIDMC (Beth Israel Deaconess Medical Center) and the Massachusetts Institute of Technology.

Funding

This study was supported by research funding from Universitas Sebelas Maret, Indonesia.

Conflict of Interest

None

References

1. Chobanian AV, Bakris GL, Black HR, Cushman WC, Green LA, et al. The Seventh Report of the Joint National Committee on Prevention, Detection, Evaluation, and Treatment of High Blood Pressure: the JNC 7 report. *JAMA*. 2003;**289**(19):2560-72. doi: 10.1001/jama.289.19.2560. PubMed PMID: 12748199.
2. Kearney PM, Whelton M, Reynolds K, Muntner P, Whelton PK, He J. Global burden of hypertension: analysis of worldwide data. *Lancet*. 2005;**365**(9455):217-23. doi: 10.1016/S0140-6736(05)17741-1. PubMed PMID: 15652604.
3. Iadecola C, Yaffe K, Biller J, Bratzke LC, Faraci FM, Gorelick PB, et al. Impact of Hypertension on Cognitive Function: A Scientific Statement From the American Heart Association. *Hypertension*. 2016;**68**(6):e67-94. doi: 10.1161/HYP.0000000000000053. PubMed PMID: 27977393. PubMed PMCID: PMC5361411.
4. Hyman L, Schachat AP, He Q, Leske MC. Hypertension, cardiovascular disease, and age-related macular degeneration. Age-Related Macular Degeneration Risk Factors Study Group. *Arch Ophthalmol*. 2000;**118**(3):351-8. doi: 10.1001/archopht.118.3.351. PubMed PMID: 10721957.
5. Zandi-Nejad K, Luyckx VA, Brenner BM. Adult hypertension and kidney disease: the role of fetal programming. *Hypertension*. 2006;**47**(3):502-8. doi: 10.1161/01.HYP.0000198544.09909.1a. PubMed PMID: 16415374.
6. El-Hajj C, Kyriacou PA. A review of machine learning techniques in photoplethysmography for the non-invasive cuff-less measurement of blood pressure. *Biomedical Signal Processing and Control*. 2020;**58**:101870. doi: 10.1016/j.bspc.2020.101870.
7. Rajput JS, Sharma M, Tan RS, Acharya UR. Automated detection of severity of hypertension ECG signals using an optimal bi-orthogonal wavelet filter bank. *Comput Biol Med*. 2020;**123**:103924. doi: 10.1016/j.compbiomed.2020.103924. PubMed PMID: 32768053.
8. Ding X, Zhang YT. Pulse transit time technique for cuffless unobtrusive blood pressure measurement: from theory to algorithm. *Biomed Eng Lett*. 2019;**9**(1):37-52. doi: 10.1007/s13534-019-00096-x. PubMed PMID: 30956879. PubMed PMCID: PMC6431352.
9. Kamal AA, Harness JB, Irving G, Mearns AJ. Skin

photoplethysmography--a review. *Comput Methods Programs Biomed.* 1989;**28**(4):257-69. doi: 10.1016/0169-2607(89)90159-4. PubMed PMID: 2649304.

10. Nuryani N, Ling SS, Nguyen HT. Electrocardiographic signals and swarm-based support vector machine for hypoglycemia detection. *Ann Biomed Eng.* 2012;**40**(4):934-45. doi: 10.1007/s10439-011-0446-7. PubMed PMID: 22012087.
11. Li J, Lu L, Zhang YH, Xu Y, Liu M, Feng K, et al. Identification of leukemia stem cell expression signatures through Monte Carlo feature selection strategy and support vector machine. *Cancer Gene Ther.* 2020;**27**(1-2):56-69. doi: 10.1038/s41417-019-0105-y. PubMed PMID: 31138902.
12. Sun J, Feng B, Xu W, editors. Particle swarm optimization with particles having quantum behavior. Proceedings of the 2004 congress on evolutionary computation (IEEE Cat No 04TH8753); Portland, OR, USA: IEEE; 2004.
13. Saeed M, Villarroel M, Reisner AT, Clifford G, Lehman LW, Moody G, et al. Multiparameter Intelligent Monitoring in Intensive Care II: a public-access intensive care unit database. *Crit Care Med.* 2011;**39**(5):952-60. doi: 10.1097/CCM.0b013e31820a92c6. PubMed PMID: 21283005. PubMed PMCID: PMC3124312.
14. Johnson AE, Pollard TJ, Shen L, Lehman LW, Feng M, Ghassemi M, et al. MIMIC-III, a freely accessible critical care database. *Sci Data.* 2016;**3**:160035. doi: 10.1038/sdata.2016.35. PubMed PMID: 27219127. PubMed PMCID: PMC4878278.
15. Liang Y, Chen Z, Ward R, Elgendi M. Hypertension Assessment via ECG and PPG Signals: An Evaluation Using MIMIC Database. *Diagnostics (Basel).* 2018;**8**(3):65. doi: 10.3390/diagnostics8030065. PubMed PMID: 30201887. PubMed PMCID: PMC6163274.
16. Elgendi M. On the analysis of fingertip photoplethysmogram signals. *Curr Cardiol Rev.* 2012;**8**(1):14-25. doi: 10.2174/157340312801215782. PubMed PMID: 22845812. PubMed PMCID: PMC3394104.
17. Zhou Z, Adeli H. Time-frequency signal analysis of earthquake records using Mexican hat wavelets. *Computer-Aided Civil and Infrastructure Engineering.* 2003;**18**(5):379-89. doi: 10.1111/1467-8667.t01-1-00315.
18. Avola D, Cinque L, Foresti GL, Lamacchia F, Marini MR, Perini L, et al. A Shape Comparison Reinforcement Method Based on Feature Extractors and F1-Score. IEEE International Conference on Systems, Man and Cybernetics (SMC); Bari, Italy: IEEE; 2019.
19. Liang Y, Chen Z, Ward R, Elgendi M. Photoplethysmography and Deep Learning: Enhancing Hypertension Risk Stratification. *Biosensors (Basel).* 2018;**8**(4):101. doi: 10.3390/bios8040101. PubMed PMID: 30373211. PubMed PMCID: PMC6316358.
20. Yang L, Sun G, Wang A, Jiang H, Zhang S, Yang Y, et al. Predictive models of hypertensive disorders in pregnancy based on support vector machine algorithm. *Technol Health Care.* 2020;**28**(S1):181-6. doi: 10.3233/THC-209018. PubMed PMID: 32364150. PubMed PMCID: PMC7369093.
21. Shi L, Duan Q, Ma X, Weng M, editors. The research of support vector machine in agricultural data classification. International Conference On Computer And Computing Technologies In Agriculture; Berlin, Heidelberg: Springer; 2011.
22. Aoyagi K, Wang H, Sudo H, Chiba A. Simple method to construct process maps for additive manufacturing using a support vector machine. *Additive Manufacturing.* 2019;**27**:353-62. doi: 10.1016/j.addma.2019.03.013.
23. Ren R, Wu DD, Liu T. Forecasting stock market movement direction using sentiment analysis and support vector machine. *IEEE Systems Journal.* 2018;**13**(1):760-70. doi: 10.1109/JSYST.2018.2794462.
24. Vogado LH, Veras RM, Araujo FH, Silva RR, Aires KR. Leukemia diagnosis in blood slides using transfer learning in CNNs and SVM for classification. *Engineering Applications of Artificial Intelligence.* 2018;**72**:415-22. doi: 10.1016/j.engappai.2018.04.024.
25. Lameski P, Zdravevski E, Mingov R, Kulakov A. SVM parameter tuning with grid search and its impact on reduction of model over-fitting. In Rough sets, fuzzy sets, data mining, and granular computing. Springer; 2015. p. 464-74.
26. Szegedy C, Liu W, Jia Y, Sermanet P, Reed S, Anguelov D, et al., editors. Going deeper with convolutions. IEEE conference on computer vision and pattern recognition; Boston, MA, USA: IEEE; 2015.
27. Tamura T, Maeda Y, Sekine M, Yoshida M. Wearable photoplethysmographic sensors—past and present. *Electronics.* 2014;**3**(2):282-302. doi: 10.3390/electronics3020282.
28. Bortolotto LA, Blacher J, Kondo T, Takazawa K, Safar ME. Assessment of vascular aging and atherosclerosis in hypertensive subjects: second derivative of photoplethysmogram versus pulse wave velocity. *Am J Hypertens.* 2000;**13**(2):165-71. doi: 10.1016/s0895-7061(99)00192-2. PubMed PMID: 10701816.

29. Charlton PH, Paliakaitė B, Pilt K, Bachler M, Zanelli S, Kulin D, et al. Assessing hemodynamics from the photoplethysmogram to gain insights into vascular age: a review from VascAgeNet. *Am J Physiol Heart Circ Physiol.* 2022;**322**(4):H493-522. doi: 10.1152/ajpheart.00392.2021. PubMed PMID: 34951543. PubMed PMCID: PMC8917928.
30. Di Maria C, Sharkey E, Klinge A, Zheng D, Murray A, O'Sullivan J, et al. Feasibility of monitoring vascular ageing by multi-site photoplethysmography. Computing in Cardiology; Krakow, Poland: IEEE; 2012.
31. Ahn JM. New Aging Index Using Signal Features of Both Photoplethysmograms and Acceleration Plethysmograms. *Healthc Inform Res.* 2017;**23**(1):53-9. doi: 10.4258/hir.2017.23.1.53. PubMed PMID: 28261531. PubMed PMCID: PMC5334132.
32. Allen J, Murray A. Effects of filtering on multisite photoplethysmography pulse waveform characteristics. Computers in Cardiology; Chicago, IL, USA: IEEE; 2004.
33. Joerger M, Huitema AD, Krähenbühl S, Schellens JH, Cerny T, Reni M, et al. Methotrexate area under the curve is an important outcome predictor in patients with primary CNS lymphoma: A pharmacokinetic-pharmacodynamic analysis from the IELSG no. 20 trial. *Br J Cancer.* 2010;**102**(4):673-7. doi: 10.1038/sj.bjc.6605559. PubMed PMID: 20125159. PubMed PMCID: PMC2837574.
34. Le J, Bradley JS, Murray W, Romanowski GL, Tran TT, Nguyen N, et al. Improved vancomycin dosing in children using area under the curve exposure. *Pediatr Infect Dis J.* 2013;**32**(4):e155-63. doi: 10.1097/INF.0b013e318286378e. PubMed PMID: 23340565. PubMed PMCID: PMC3632448.
35. Baek HJ, Kim JS, Kim YS, Lee HB, Park KS, et al. Second derivative of photoplethysmography for estimating vascular aging. 6th International Special Topic Conference on Information Technology Applications in Biomedicine; Tokyo, Japan: IEEE; 2007.
36. Miyai N, Miyashita K, Arita M, Morioka I, Kamiya K, Takeda S. Noninvasive assessment of arterial distensibility in adolescents using the second derivative of photoplethysmogram waveform. *Eur J Appl Physiol.* 2001;**86**(2):119-24. doi: 10.1007/s004210100520. PubMed PMID: 11822470.
37. Elgendi M, Jonkman M, De Boer F. Heart Rate Variability Measurement using the Second Derivative Photoplethysmogram. Proceedings of the Third International Conference on Bio-inspired Systems and Signal Processing; Valencia, Spain: INSTICC Press; 2010.
38. Otsuka T, Kawada T, Katsumata M, Ibuki C. Utility of second derivative of the finger photoplethysmogram for the estimation of the risk of coronary heart disease in the general population. *Circ J.* 2006;**70**(3):304-10. doi: 10.1253/circj.70.304. PubMed PMID: 16501297.
39. Raj S, Ray KC, Shankar O. Development of robust, fast and efficient QRS complex detector: a methodological review. *Australas Phys Eng Sci Med.* 2018;**41**(3):581-600. doi: 10.1007/s13246-018-0670-7. PubMed PMID: 30117043.
40. Tan L, Jiang J. Digital signal processing: fundamentals and applications. Academic Press; 2018.